Eur. Phys. J. B **29**, 27–33 (2002)
DOI: 10.1140/epjb/e2002-00258-x

THE EUROPEAN PHYSICAL JOURNAL B

Electronic localization in an extreme 1-D conductor: the organic salt (TTDM-TTF)$_2$ [Au(mnt)$_2$]

E.B. Lopes[1], H. Alves[1], E. Ribera[2], M. Mas-Torrent[2], P. Auban-Senzier[3], E. Canadell[2], R.T. Henriques[1,4], M. Almeida[1,a], E. Molins[2], J. Veciana[2], C. Rovira[2], and D. Jérome[3]

[1] Instituto Tecnológico e Nuclear, 2686-953 Sacavém, Portugal
[2] Institut de Ciència de Materials de Barcelona (CSIC), Campus de la UAB, 08193 Bellaterra, Spain
[3] Laboratoire de Physique des Solides, Université Paris-Sud[b], 91405 Orsay, France
[4] Instituto Superior Técnico, 1049-001 Lisboa, Portugal

Received 15 April 2002 / Received in final form 17 June 2002
Published online 17 September 2002 –

Abstract. This article reports the investigation of a new low-dimensional organic salt, (TTDM-TTF)$_2$ [Au(mnt)$_2$], by single crystal X-ray diffraction, static magnetic susceptibility, EPR, thermopower, electrical resistivity measurements under pressure up to 25 kbar and band structure calculations. The crystal structure consists in a dimerized head to tail stacking of TTDM-TTF molecules separated by layers of orthogonal Au(mnt)$_2$ anions. The absence of overlap between neighboring chains coming from this particular crystal structure leads to an extreme one-dimensionality (1-D) for which the carriers of the half-filled conduction band become strongly localized in a Mott-Hubbard insulating state. This material is the first 1-D conductor in which the Mott-Hubbard insulating character cannot be suppressed under pressure.

PACS. 72.80.Le Polymers; organic compounds – 72.20.Pa Thermoelectric and thermomagnetic effects

1 Introduction

The study of quasi one dimensional molecular systems has revealed a very rich (pressure, temperature) phase diagram. Most often, as in Bechgaard salts, (TMTSF)$_2$X and their sulfur analogues, the Fabre salts (TMTTF)$_2$X, the application of a pressure increases the transverse coupling $t_\perp$ between the partially oxidized stacks, leading to an increased dimensionality of the system. The typical situation encountered in (TMTTF)$_2$X salts at low pressure, namely a high temperature Mott localization regime associated to a spin-Peierls ground state at low temperature, evolves, either through a change of compound in the Fabre-Bechgaard series or under pressure, towards a high temperature metallic regime giving rise to spin density wave or superconducting ground states at low temperature. A generic phase diagram has thus been proposed for this (TM)$_2$X family where TM labels either TMTTF or its selenide analog TMTSF [1] .

Due to the breakdown of the Fermi liquid theory in 1-D, a Luttinger liquid description is favored at low pressure, characterized by the decoupling of charge and spin degrees of freedom, the absence of any discontinuity in the quasiparticule distribution function at the Fermi level and a power law decay at long distance of the spin and charge correlation functions. However, because of the commensurate band filling of these materials a Mott-Hubbard insulating regime is predicted to occur in the strong coupling limit. Hence, we can expect the restoration of an anisotropic Fermi liquid under pressure when $t_\perp$ is enhanced with the concomitant weakening of the Coulomb coupling.

Therefore, the study of the pressure-temperature phase diagram and of the dimensionality crossover in organic systems has attracted a great deal of interest. In this paper, we report the synthesis and the study of a new molecular conducting system, based on an asymmetric TTF derivative, the π-electron donor thiophenothiodimethylene-tetrathiafulvalene (TTDM-TTF). This system, in spite of some structural analogy with (TMTTF)$_2$X and (TMTSF)$_2$X salts, exhibiting stacks of donors arranged in layers with short interchain contacts, shows a unique extreme 1-D character accompanied by a strong electronic localization, which is extremely robust to pressures as high as 25 kbar. This experimental behavior fits rather well with recent theoretical results.

2 Experimental

(TTDM-TTF)$_2$[Au(mnt)$_2$] was synthesized by electrocrystallization from the new π-electron donor

[a] e-mail: malmeida@itn.pt
[b] UMR 8502 CNRS

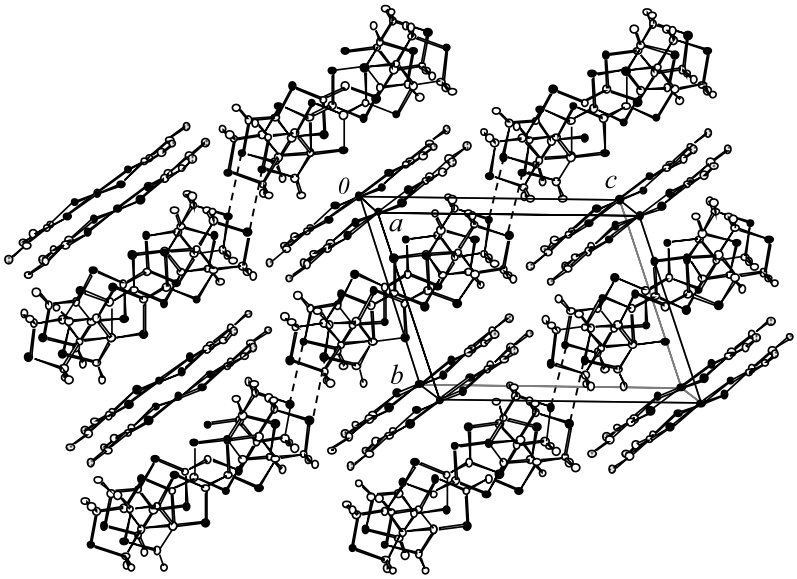

Fig. 1. $(TTDM\text{-}TTF)_2$ $[Au(mnt)_2]$ structure. The dashed lines denote the short S···S contacts.

thiophenothiodimethylene-tetrathiafulvalene (TTDM-TTF) [2] with the tetrabutylammonium salt of the bis-maleonitriledithiolate (mnt) Au(III) complex. Single crystals of $(TTDM\text{-}TTF)_2[Au(mnt)_2]$ with typical dimensions, $1.5 \times 0.7 \times 0.08$ mm^3 were obtained using galvanostatic conditions ($\approx 1\mu$A/cm^2) for about 8 days, on platinum electrodes from solutions of TTDM-TTF and $(n\text{-}Bu_4N)Au(mnt)_2$ in CH_2Cl_2.

Electrical resistivity and thermopower measurements at ambient pressure were performed along the long axis (**a**) of the needle shaped crystals under vacuum in the range 100–310 K, using a cell attached to the cold stage of a closed cycle helium refrigerator. Electrical resistivity was measured by a four contact method using an AC current of 1 μA at 77 Hz, the voltage being measured by a lock-in amplifier (EG&G Par 5316). The thermopower was measured by a slow AC ($\approx 10^{-2}$ Hz) technique [3] using thermal gradients below 1 K, as previously described [4] . In both measurements the sample was attached to gold wires ($\phi = 25$ μm) with platinum paint (Demetron 308A) and the absolute thermopower of the sample was calculated after correction for the absolute thermopower of the gold wires using the data of Huebner [5].

In a second step, the electrical resistivity was studied in the same configuration under hydrostatic pressure up to 25 kbar using a non-magnetic NiCrAl high pressure clamp cell with silicon oil as the pressure transmitting medium. The pressure inside the cell was calibrated at room temperature by a manganin gauge.

The static magnetic susceptibility of polycrystalline samples, was measured in the temperature range 4–300 K using a Faraday system (Oxford Instruments) equipped with a 7 T superconducting magnet. The measurements were performed under a static magnetic field of 2 and 5 T, the force on the samples, contained in a previously measured thin-walled Teflon bucket, being measured with a microbalance (Sartorius S3D-V) applying forward and reverse gradients of 5 T/m. The paramagnetic susceptibility was calculated considering a diamagnetic correction, estimated from tabulated Pascal constants as 4.9×10^{-4} emu/mol.

EPR spectra in the range 4–300 K were obtained with an X-Band Bruker ESP 300E spectrometer equipped with a rectangular cavity operating in T102 mode, a Bruker variable temperature unit and an Oxford EPR-900 cryostat, a Field Frequency lock ER 033M system and a NMR Gaussmeter ER 035M. The modulation amplitude was kept well below the line width and the microwave power was well below saturation.

3 Results

The $(TTDM\text{-}TTF)_2[Au(mnt)_2]$ compound crystallizes in the triclinic $P\overline{1}$ system [6] and the asymmetric molecular unit comprises one TTDM-TTF donor unit and one half Au complex anion. The structure of $(TTDM\text{-}TTF)_2[Au(mnt)_2]$ (see Fig. 1) consists in stacks of the TTDM-TTF units along the **a**-axis and $Au(mnt)_2$ anions which are almost perpendicular to the donors. The donor molecules present a zigzag head to tail stacking pattern, with interplanar distances of 3.474 Å and 3.524 Å, which are very similar to the structure of the $(TMTSF)_2X$ salts [7]. However, in contrast to the latter compounds, in $(TTDM\text{-}TTF)_2[Au(mnt)_2]$, the gold complex anions separate the donor chains along the **b**-axis preventing the formation of any lateral contact between donors. Nevertheless, structural layers are formed in which the donor stacks are connected to each other along **c**-**b** by very short S···S contacts (3.398 Å) (see Fig. 1). In spite of the short contacts mentioned above, it should be kept in mind that one of the sulfur atoms involved in these contacts does not participate at all in the HOMO of the molecule since the CH_2 groups in the thiodimethylen-substituent of the

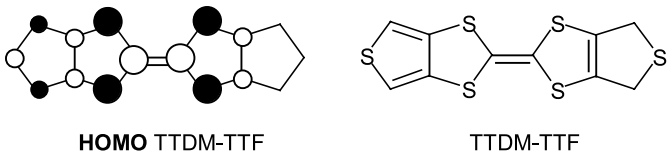

Fig. 2. Highest occupied molecular orbital (HOMO) (left) and molecular structure (right) diagrams of the TTDM-TTF donor.

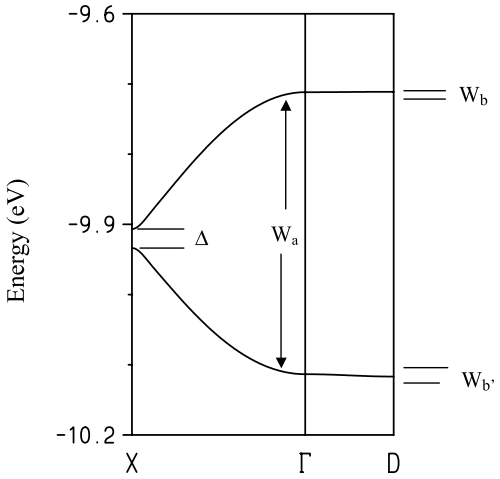

Fig. 3. Calculated band structure for the TTDM-TTF donor layers in (TTDM-TTF)$_2$[Au(mnt)$_2$]. Γ, X and D refer to the (0, 0), ($a^*/2$, 0) and (0, $d^*/2$) wave vectors with $d = (c - b)$.

TTF core break the conjugation and separate the terminal S atom from the central π-system (see Fig. 2). Therefore, these contacts are not expected to provide any significant electronic two-dimensionality to this compound. Consequently, these two peculiarities of the TTDM-TTF structure are likely to provide a unique 1-D character to this organic salt.

Furthermore, the perfect electronic isolation of the stacks is also supported by the band structure calculations for the TTDM-TTF layers (see Fig. 3), which show the absence of any dispersion perpendicularly to the stacks direction. The tight-binding band structure calculations were based upon the effective one-electron Hamiltonian of the extended Hückel method [8]. The off-diagonal matrix elements of the Hamiltonian were calculated according to the modified Wolfsberg-Helmholz formula [9]. All valence electrons were explicitly taken into account in the calculations and the basis set consisted of single-ζ Slater-type orbitals for C 2s and 2p, S 3s and 3p and H 1s. The exponents, contraction coefficients and atomic parameters were taken from previous work [10].

The 2:1 stoichiometry of the compound would lead in principle to a three-quarter filled band but the presence of a structural dimerization along the donor stacks implies the opening of a gap in the middle of the band which in turn becomes effectively half-filled (see Fig. 3). If a metallic filling of the band is assumed, the associated Fermi surface is made of just two nearly straight lines perpendicular to the chains direction corresponding to an almost perfect

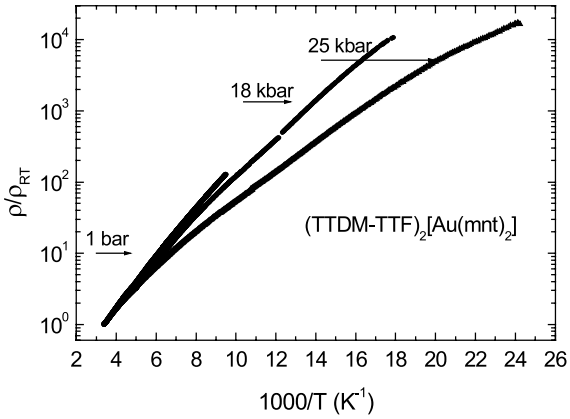

Fig. 4. Electrical resistivity of (TTDM-TTF)$_2$ [Au(mnt)$_2$] measured along **a** at different pressures as a function of the reciprocal temperature.

1-D system. Inclusion of the Au(mnt)$_2$ acceptors in the calculations does not change the situation of a nearly perfect 1-D conductor. The absence of any dispersion in the direction perpendicular to the chains was also confirmed by using more spatially extended orbitals of double-ζ type quality for the C and S atoms.

It is useful to compare the main results of the band structure calculations – $W_a = 0.402$ eV, $\Delta = 0.027$ eV, $W_b = 0.0005$ eV, $W_{b'} = 0.003$ eV (see Fig. 3 for labeling) – with those obtained using the same computational approach for (TMTTF)$_2$Br [11] – $W_a = 0.354$ eV, $\Delta = 0.027$ eV, $W_b = 0.030$ eV, $W_{b'} = 0.082$ eV –. While the dimerization gap (Δ) is of the same order for both compounds, in (TTDM-TTF)$_2$ [Au(mnt)$_2$], the band dispersion along the chains (W_a) is slightly larger than in (TMTTF)$_2$Br and there is no dispersion at all perpendicularly to the chains (W_b , $W_b' \approx 0$). On the basis of a non- interacting electron band picture, we should expect a metallic conductivity for the present salt at high temperature, as observed in (TMTTF)$_2$Br down to 80 K. However, the extreme one dimensionality of the system together with the effect of strong interactions may result in an electronic localization even at room temperature as discussed in the following section.

Electrical conductivity measurements of this material performed along **a**-axis on six different samples give values ranging between 0.15 and 1 Scm^{-1} at room temperature with a similar semiconducting behavior for all samples upon cooling. This relatively large dispersion of conductivity values could be ascribed to variations in sample quality. The resistivity, ρ, measured as a function of temperature, T, presents a variation of log ρ *vs.* $1/T$ close to linearity between 300 and 100 K, with an activation energy of $E_a = 900$ K around room temperature, slightly decreasing upon cooling, as it can be seen in Figure 4.

The thermopower of (TTDM-TTF)$_2$ [Au(mnt)$_2$] has been measured at ambient pressure as a function of the temperature (Fig. 5). It is positive, $S \approx 73$ μV/K at room temperature in agreement with hole transport and decreases upon cooling. This behavior resembles that

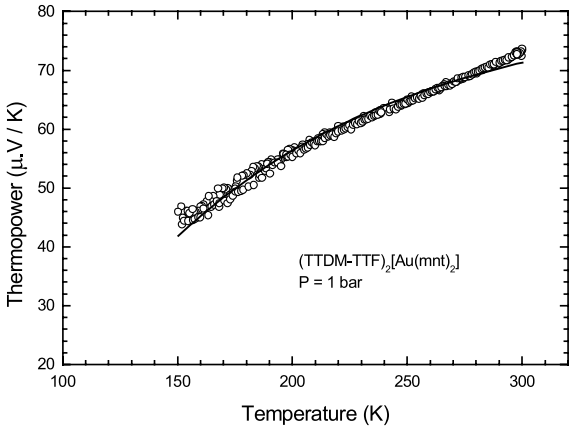

Fig. 5. Absolute thermopower of $(TTDM\text{-}TTF)_2$ $[Au(mnt)_2]$ measured along **a** as a function of the temperature. The line is a fit to equation 1 with $W_E = 325$ K (see text).

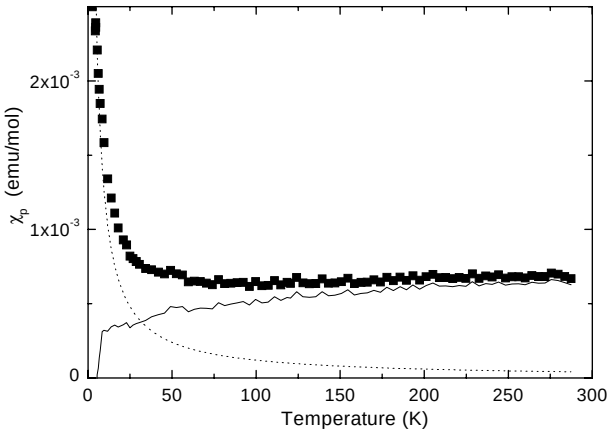

Fig. 6. Static paramagnetic susceptibility χ_p of $(TTDM\text{-}TTF)_2$ $[Au(mnt)_2]$ measured in a polycrystalline sample as a function of the temperature: The lines are a decomposition in a Curie tail, corresponding to $\approx 3\%$ of $S = 1/2$ spins (dotted line) and the intrinsic susceptibility (full line).

obtained in usual metals when the Fermi level lies in a continuum of states, but in view of the activated conductivity results, it cannot be ascribed to a metallic regime.

The paramagnetic susceptibility measured in polycrystalline samples amounts to 1.0×10^{-3} emu/mol at room temperature and is only weakly temperature dependent down to ≈ 40 K. At lower temperature, it increases and becomes dominated by a Curie tail ascribed to impurities and defects, corresponding to $\approx 3.3\%$ of $S = 1/2$ spins. Taking into account this Curie tail, the estimated intrinsic susceptibility of this compound shows a sharp decrease around 10 K (see Fig. 6) which could possibly be ascribed to a spin-Peierls transition (see for instance the ESR spin susceptibility results on $(TMTTF)_2PF_6$ [12], or $(BCPTTF)_2X$ [13] and reference [14] for a review).

EPR spectra in single crystals at room temperature present a single line at g-values in the range 2.0128–2.0020 depending on the sample orientation with respect to the

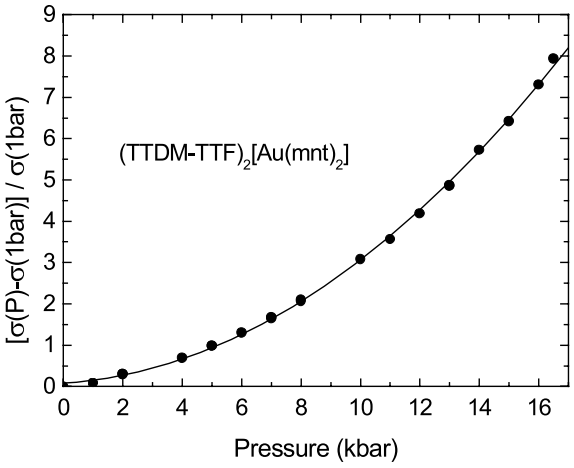

Fig. 7. Room temperature pressure dependence of the electrical conductivity of $(TTDM\text{-}TTF)_2$ $[Au(mnt)_2]$ measured along **a**-axis.

external magnetic field. These g-values are typical of TTF derivatives and confirm that the $Au(mnt)_2$ complex remains in the monoanionic diamagnetic state. The linewidths are very similar in all orientations of the sample (9.5–11.5 G) being small and consistent with the 1-D character of the electronic system. The linewidth decreases monotonically with temperature until 15 K where the value is 0.6 Gauss and then increases slowly reaching 0.9 G at 4 K. The intensity of the line follows the same temperature dependence as that observed for the static magnetic susceptibility.

The longitudinal resistivity of $(TTDM\text{-}TTF)_2$ $[Au(mnt)_2]$ has been studied up to 25 kbar. We first notice a very strong pressure coefficient of the conductivity at room temperature which can be modeled by an exponential pressure dependence (Fig. 7) at variance with the usual linear pressure dependence of 50% $kbar^{-1}$ and 25% $kbar^{-1}$ observed in $(TMTTF)_2X$ and $(TMTSF)_2X$ compounds respectively. The behavior of $(TTDM\text{-}TTF)_2$ $[Au(mnt)_2]$ is actually closer to the situation encountered in the ordered sulfur selenium solid solution $[(TMTTF)_{0.5}(TMTSF)_{0.5}]_2ReO_4$ [15] which exhibits a far more insulating character than the homomolecular $(TMTTF)_2ReO_4$ salt [16]. The striking behavior of $(TTDM\text{-}TTF)_2$ $[Au(mnt)_2]$ is that in spite of the very large increase of the conductivity under pressure at room temperature, the usual pressure-induced crossover from insulating to metallic behavior in the Fabre-Bechgaard salts is not observed (see Fig. 4). Therefore, the insulating character of the present compound is very robust to the application of a pressure. This feature is illustrated in Figure 8 showing the pressure dependence of the activation energy E_a, which can be derived from the Arrhenius plot ($\log(\rho/\rho_0) = E_a/T$) around room temperature in $(TTDM\text{-}TTF)_2$ $[Au(mnt)_2]$, together with the values obtained in $[(TMTTF)_{0.5}(TMTSF)_{0.5}]_2ReO_4$ [17] and $(TMTTF)_2PF_6$ [18] which are both strongly pressure dependent.

While the activation energy measured in the high temperature regime ($3 < 1000/T < 6$), *i.e.* in a temperature

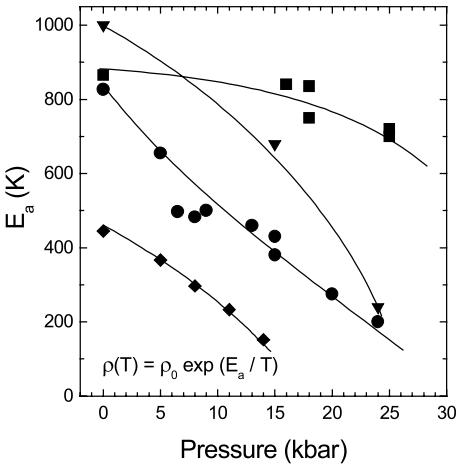

Fig. 8. Pressure dependence of the resistivity activation energy E_a derived from the high temperature fits in (TTDM-TTF)$_2$[Au(mnt)$_2$] (squares), compared with the values obtained in [(TMTTF)$_{0.5}$(TMTSF)$_{0.5}$]$_2$ReO$_4$ (circles), (TMTTF)$_2$PF$_6$ (triangles) and (DT-TTF)$_2$ Au(mnt)$_2$] (diamonds).

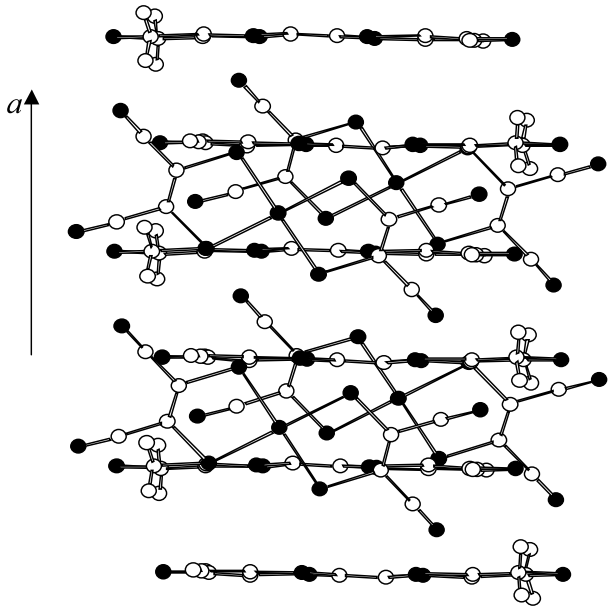

Fig. 9. View perpendicular to the TTDM-TTF chains showing the location of the Au(mnt)$_2$ acceptors around such a chain.

window smaller than the gap itself, is only very weakly affected by pressure, decreasing from 900 K at ambient pressure to 700 K under 25 kbar, the low temperature activation energy exhibits some pressure dependence although not large (see Figs. 4 and 8).

4 Discussion

The major result of the present work is the robustness of the activation energy to the application of pressure which is *at variance* with the decrease observed in all members of the Fabre-Bechgaard series. In addition, the temperature dependence of the thermopower which is reminiscent of that observed in a metal requires a special interpretation.

In order to comment on the strongly pressure-resistant insulating character it is interesting to compare the pressure dependence of the activation energy of (TTDM-TTF)$_2$ [Au(mnt)$_2$] to that measured in (TMTTF)$_2$PF$_6$, and also [(TMTTF)$_{0.5}$(TMTSF)$_{0.5}$]$_2$ReO$_4$, ((S − Se)$_2$ ReO$_4$), see Figure 8. The compound (S-Se)$_2$ReO$_4$ in which a large activation energy has been measured is quite particular. As this ordered heteromolecular solid solution exhibits an alternation of TMTTF and TMTSF molecules along the three crystallographic directions, the on-site energies of close neighbors molecules become inequivalent and the potential seen by the electrons at the wave vector $4k_F$ acquires a component provided by the difference in on-site energies [15]. This $4k_F$ site potential leads in turn to the Mott-Hubbard localization. Such a contribution would however not be present in a homomolecular salt such as (TMTTF)$_2$PF$_6$. In this latter salt the Mott-Hubbard gap may come from the 4k$_F$ bond potential (dimerization) or from the role of the Umklapp scattering in the quarter-filled band situation. The crystal structure of (TTDM-TTF)$_2$ [Au(mnt)$_2$] is quite different from that of the Fabre-Bechgaard series since along the stacking direction there exists an alternation of intermolecular bonds facing and not facing the potential created by the anions (see Fig. 9). This anion potential may thus be at the origin of the bond modulation and consequently of the structural modulation accompanied by a dimerization gap in the (TTDM-TTF)$_2$ [Au(mnt)$_2$] band structure. Unless a severe structural transition occurs under pressure we cannot expect much effect of pressure in reducing the bond modulation.

Furthermore, a major feature of (TTDM-TTF)$_2$ [Au(mnt)$_2$] is the absence of any bare interstack coupling along both transverses directions as already mentioned in Section 3. We think the absence of transverse coupling in (TTDM-TTF)$_2$ [Au(mnt)$_2$] *at variance* with the existence of a significant coupling along **b** in the Fabre-Bechgaard series is a clue to understand the robustness of the Mott-Hubbard insulating state against pressure. The Mott-Hubbard gap is the result of the Umklapp scattering processes of the electrons in the case of a commensurate band filling. Provided the electron-electron interaction is weakly or strongly repulsive in the case of half-filled or quarter-filled bands respectively a Mott-Hubbard gap opens at the Fermi level of isolated stacks with a concomitant confinement of the carriers on individual chains. However, it is known that the existence of a finite interstack hopping results in a crossover between the Mott-Hubbard insulating regime and a metallic Luttinger regime. Recent calculations of the deconfinement transition using the dynamical mean field theory [19] have located the deconfinement crossover at the critical value of the interchain coupling corresponding to $t_\perp/w \approx 0.05$ where w is the bandwidth. This critical value of the transverse interaction which is indeed very close to the results of the calculation for the band parameters in the Fabre-Bechgaard

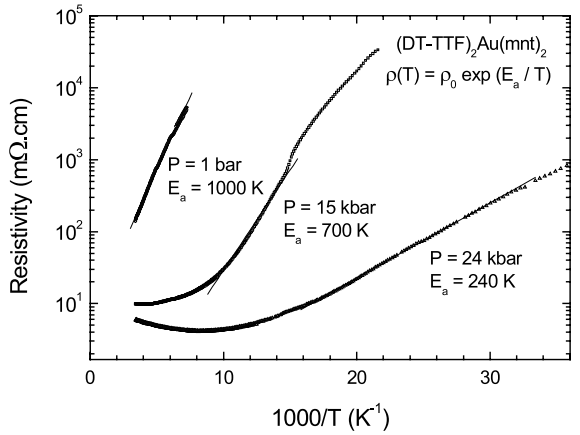

Fig. 10. Electrical resistivity of (DT-TTF)$_2$ [Au(mnt)$_2$] measured along **a** at different pressures as a function of the reciprocal temperature.

series could explain why the Mott-Hubbard insulating state can be easily destabilized under pressure. However, band structure calculations lead to an interchain interaction which is essentially zero in (TTDM-TTF)$_2$ [Au(mnt)$_2$], *i.e.* much smaller than the critical value for deconfinement. Since this coupling is not expected to be significantly enhanced under pressure we do not find surprising that the Mott-Hubbard insulating character remains up to 25 kbar.

At this stage it is illuminating to compare the properties of (TTDM-TTF)$_2$ [Au(mnt)$_2$] with those of an other radical ion salt made of the donor DT-TTF together with the Au(mnt)$_2$ anion, *i.e.* (DT-TTF)$_2$ [Au(mnt)$_2$] [20]. At variance with the situation encountered in TTDM-TTF molecules, the sulfur atoms located at both ends of the DT-TTF molecules belong to the π-electron system of the entire molecule. Consequently, significant interstack interactions are likely to be established *via* these short S...S contacts between neighboring stacks of donor molecules. The structure of (DT-TTF)$_2$ [Au(mnt)$_2$] is somewhat particular as it comprises pairs of strongly interacting chains forming two-leg ladders which are interacting *via* the S$\cdots$S interladder contacts (typically $t_\perp/w \approx 0.04$ for the interladder interaction). The response of this material to pressure reveals an efficient suppression of the insulating character under pressure [21]. As displayed in Figure 10, the activation energy drops roughly by a factor 5 under 24 kbar. This is reminiscent of the behavior observed in the (S-Se)$_2$ReO$_4$ compound belonging to the Fabre-Bechgaard series which presents a similar activation energy around 1000 K under ambient pressure.

We come now to the interpretation of the Seebeck coefficient displayed in Figure 5. At first sight, the temperature dependence of the Seebeck coefficient resembles that of metals but this interpretation can be ruled out on account of the strongly insulating character revealed by the conductivity data. Second, similar behaviors of Seebeck coefficients have been measured in the past for certain insulating salts of the ion-radical tetracyanoquinodimethane, TCNQ [22]. The thermopower based on the motion of interacting carriers moving from site to site *via* thermally activated jumps, proposed by Burarov *et al.* [23], leads to a temperature dependence (*i.e.* positive temperature coefficient) in fair agreement with the data of these materials [22]. It is tempting to use the same model for the thermopower to fit the data of (TTDM-TTF)$_2$ [Au(mnt)$_2$]. In case of one hole for every two molecules the Seebeck coefficient according to this model reads [23]:

$$S = \frac{k}{|e|}\left[\ln\left(1+\exp\overline{W}\right) - \frac{\overline{W}\exp\overline{W}}{1+\exp\overline{W}}\right] \qquad (1)$$

where $\overline{W} = \frac{W_E}{kT}$, with W_E being the energy difference of bonds with one empty site and zero empty site in between the holes. As shown in Figure 5, the quality of the fit for a half-filled band system with $W_E \approx 325$ K seems to be satisfactory. However, this picture relies on a model for transport based on thermally activated hopping between localized electronic states. This model has been largely discussed in the seventies in relation with the early low dimensional conductors [22]. As far as transport is concerned, the hopping model leads to the $\log \rho \sim (T/T_0)^{1/2}$ law in one dimension [24]. However, the hopping model has been opposed by a correlation-induced 1D localization due to the strong electron-electron repulsion [25]. More recently, the dominant role of correlations in 1D organic conductors has been firmly established by the signature of $4k_F$ scattering in diffuse X rays experiments [26]. Since the structure of the present salt (TTDM-TTF)$_2$ [Au(mnt)$_2$] does not show any sign of disorder (shown however in the mixed valence salts of TCNQ) we can be confident that the insulating nature of (TTDM-TTF)$_2$ [Au(mnt)$_2$] can be attributed to a 1D Mott insulator. We believe that the close resemblance of transport and thermopower data with the hopping model is accidental. It is well known from the study of the Fabre-Bechgaard series in which the Mott insulator model is not disputed that the activation law for the resistivity is never followed accurately down to low temperature. Furthermore the study of the thermopower in the (TMTTF)$_2$X series varying the anion X [27] and in the solid solution [(TMTSF)$_{1-x}$ (TMTTF)$_x$]$_2$PF$_6$ [28] has shown that, although its value at room temperature is always in the range of 40 to 50 μV/K, the temperature variation on cooling is very much system dependent. Therefore, we must take the interpretation of the Seebeck coefficient of the present compound with a grain of salt.

5 Conclusion

Band structure calculations of the organic salt (TTDM-TTF)$_2$ [Au(mnt)$_2$] lead to an extreme 1-D character due to the absence of electronic interchain interactions *via* terminal sulfur contacts and also to the peculiar structural arrangement of the anions, located nearly perpendicular to the donor stacks. Consequently, (TTDM-TTF)$_2$ [Au(mnt)$_2$] represents a unique compound among 1-D conductors remaining 1-D even under high pressure and contrasting with the members of the Fabre-Bechgaard series in which the finite interchain coupling can be modified

(increased) under pressure. The Mott-Hubbard insulating nature of $(TTDM\text{-}TTF)_2$ $[Au(mnt)_2]$ persists up to pressures of 25 kbar which are usually high enough to severely decrease (if not suppress) the localization in the Fabre-Bechgaard series.

The comparison between the pressure response of various radical cation salts based on TM, DT-TTF and TTDM-TTF donor molecules strongly suggests that the coupling between chains or ladders in $(TM)_2$ X and $(DT\text{-}TTF)_2$ X compounds respectively is a relevant parameter allowing the crossover between the Mott-Hubbard behavior and a Fermi-like behavior to be observed under high pressure in the Fabre- Bechgaard series of organic conductors.

This work was partially supported by Fundação para a Ciência e Tecnologia (Portugal) under contracts POCTI/1999/CTM/35452, and by DGI (Spain) (BQU2000-1157 and BFM2000-1312-C02-01) and Generalitat de Catalunya (2001SGR-362 and 2001SGR-333). The collaboration between the team members of Sacavém and Barcelona was supported under the CSIC-ICCTI bilateral agreement and by COST action D14. P.A. and D.J. wish to acknowledge useful discussions with S. Biermann.

References

1. D. Jérome, Science **252**, 1509 (1991); C. Bourbonnais, D. Jérome, *Adv. in Synthetic Metals*, edited by P. Bernier, S. Lefrant, G. Bidan (Elsevier, 1999)
2. The thiophenothiodimethylene-tetrathiafulvalene (TTDM -TTF) donor was prepared by cross-coupling $P(OMe)_3$ mediated reaction of [3,4-d]-1,3-dithiol-2-thione [P. Shu, L-Y. Chiang, T. Emge, D. Holt, T. Kistenmacher, M. Lee, J. Stokes, T. Poehler, A. Bloch, D. Cowan, J. *Org. Chem. 49*, 1117 (1984)] and 4,6-dihydrothieno[3,4-d]-1,3-dithiol-2- thione [C. Rovira, J. Veciana, N. Santaló, J. Tarrés, J. Cirujeda, E. Molins, J. Llorca, E. Espinosa, J. Org. Chem. **59**, 3307 (1994)]
3. P.M. Chaikin, J.F. Kwak, Rev. Sci. Instrum. **46**, 218 (1975)
4. M. Almeida, S. Oostra, L. Alcácer, Phys. Rev. B **30**, 2839 (1984)
5. R.P. Huebner, Phys. Rev. A **135**, 1281 (1964)
6. Crystallographic data for $C_{28}H_{12}N_4S_{16}Au$: crystal dimensions $0.70 \times 0.10 \times 0.08$ mm^3; $M = 1114.34$, triclinic, space group $P\bar{1}$, $a = 6.999(2)$ Å, $b = 10.054(8)$ Å, $c = 13.234(12)$ Å, $\alpha = 71.19(10)^\circ$, $\beta = 82.41(5)^\circ$, $\gamma = 84.29(4)^\circ$; $Z = 1$; $V = 872(11)$ Å^3, $\rho_{calc} = 2.122$ g cm^{-3}. Data were collected at 293 (2) K on an Enraf-Nonius CAD4 diffractometer equipped with a Mo X-ray tube and a graphite monochromator to select the Mo_K radiation (absorption coefficient $\mu = 5.208$ mm^{-1}). Data collection up to $2\theta = 61^\circ$ and $-9 \leq h \leq 9$, $-13 \leq k \leq 5$, $0 \leq l \leq 18$ affords 5298 reflections measured with $\omega - 2\theta$ scans. At convergence the final R indices were $R_1 = 0.0886$, $wR_2 = 0.1131$ (for all data) and $R_1 = 0.0429$, $wR_2 = 0.0996$ (for $I > 2\sigma(I)$ reflections). The final max/min residuals were 1.285/–1.746 e Å^3
7. N. Thorup, G. Rindorf, H. Soling, K. Bechgaard, Acta Cryst. B **37**, 1236 (1981)
8. M.-H. Whangbo, R. Hoffmann, J. Am. Chem. Soc. **100**, 6093 (1976)
9. J. Ammeter, H.-B- Bürgi, J. Thibeault, R. Hoffmann, J. Am. Chem. Soc. **100**, 3686 (1976)
10. E. Canadell, I.E.-I. Rachidi, S. Ravy, J.P. Pouget, L. Brossard, J.-P. Legros, J. Phys. France **50**, 2967 (1989)
11. L. Balicas, K. Behnia, W. Kang, E. Canadell, P. Auban-Senzier, D. Jérome, M. Ribault, J.M. Fabre, J. Phys. I France **4**, 1539 (1994)
12. F. Creuzet, thesis, Orsay, 1981
13. Q. Liu, S. Ravy, J.-P. Pouget, C. Coulon C. Bourbonnais, Synth. Met. **55-57**, 1840 (1993)
14. M. Dumm, A. Loidl, B.W. Fravel, K.P. Starkey, L.K. Montgomery, M. Dressel, Phys. Rev. B **61**, 511 (2000)
15. V. Ilakovac, S. Ravy, J.P. Pouget, C. Lenoir, K. Boubekeur, P. Batail, S. Dolanski Babic, N. Biskup, B. Korin-Hamzic, S. Tomic, Phys. Rev. B **50**, 7136 (1994)
16. S. Tomic, P. Auban-Senzier, D. Jérome, Synth. Met. **103**, 2197 (1999)
17. P. Auban-Senzier, C. Lenoir, P. Batail, D. Jérome, S. Tomic, Eur. Phys. J. B **7**, 529 (1999)
18. J. Moser, M. Gabay, P. Auban-Senzier, D. Jérome, K. Bechgaard, J. M. Fabre, Eur. Phys. J. B **1**, 39 (1998)
19. S. Biermann, A. Georges, A. Lichtenstein, T. Giamarchi, Phys. Rev. Lett. **87**, 276405 (2001) and `cond-mat/0201542`
20. E. Ribera, C. Rovira, J. Veciana, J. Tarrés, E. Canadell, R. Rousseau, E. Molins, M. Mas, J.P. Schoeffel, J.P. Pouget, J. Morgado, R.T. Henriques, M. Almeida, Chem. Eur. J. **5**, 2025 (1999)
21. E.B. Lopes, R.T. Henriques, M. Almeida, E. Ribera, M. Mas-Torrent, J. Veciana, C. Rovira, P. Auban-Senzier, D. Jérome, *Proceedings of the fourth International Symposium on Crystalline Organic Metals, Superconductors and Ferromagnets, ISCOM 2001 (Japan)*, Synth. Met. (Elsevier), to be published (2002)
22. I.F. Schegolev, Phys. Stat. Sol.(a) **12**, 9 (1972)
23. L.I. Burarov, D.N. Fedutin, I.F. Schegolev, Sov. Phys. JETP **32**, 612 (1971)
24. A.N. Bloch, R.B. Weisman, C.M. Varma, Phys. Rev. Lett. **28**, 753 (1972)
25. A.J. Epstein, S. Etemad, A.F. Garito, A.J. Heeger, Solid State Commun. **9**, 1803 (1971)
26. J.-P. Pouget in *Semiconductors and semimetals* (Academic Press, 1988)
27. K. Mortensen, E.M. Conwell, J.-M. Fabre, Phys. Rev. B **28**, 5856 (1983)
28. K. Mortensen, E.M. Engler, Phys. Rev. B **29**, 842 (1984)